

Supplementary Materials

NIR-Triggered Logic Gate in MXene-Modified Perovskite Resistive Random Access Memory

Rongbin Li,^{a,†} Yan Sun,^{a,†} Qianyu Zhao,^a Xin Hao,^a Haowei Liang,^a Shengang Xu,^{a,b}
Yingliang Liu,^{*ab} Xiaoman Bi,^{*ab} Shaokui Cao,^{ab}

^aSchool of Materials Science and Engineering, Zhengzhou University, Zhengzhou 450001, People's Republic of China

^bHenan Key Laboratory of Advanced Nylon Materials and Application, Zhengzhou university, Zhengzhou 450001, People's Republic of China

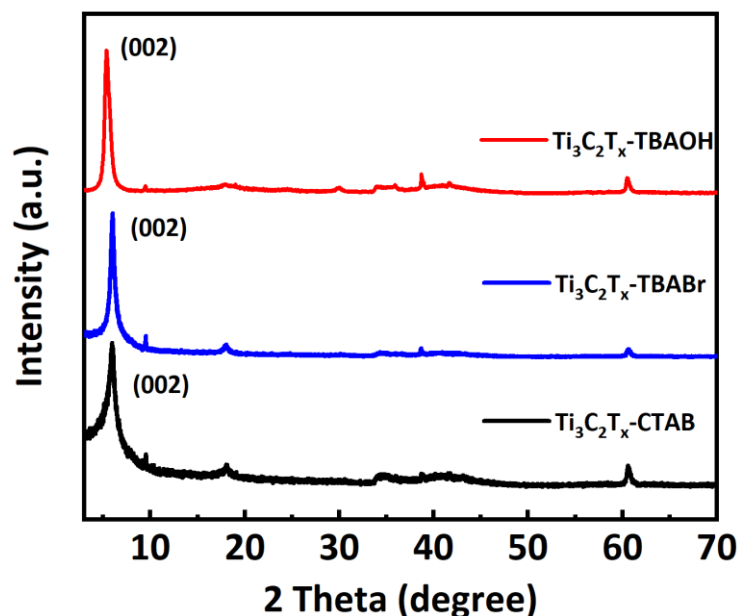


Fig. S1 XRD patterns of Ti₃C₂T_x-TBAOH, Ti₃C₂T_x-TBABr, Ti₃C₂T_x-CTAB.

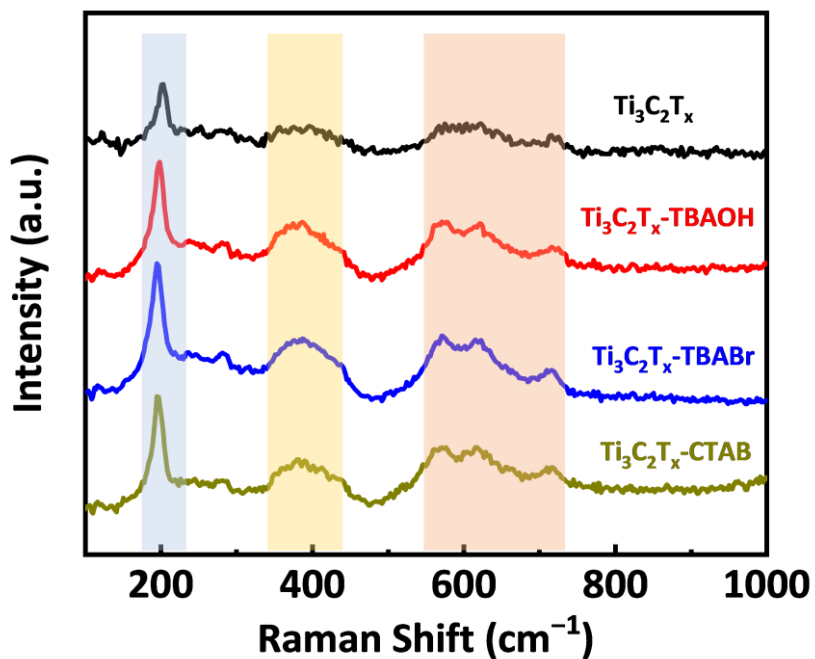


Fig. S2 Raman spectra of $\text{Ti}_3\text{C}_2\text{T}_x$, $\text{Ti}_3\text{C}_2\text{T}_x\text{-TBAOH}$, $\text{Ti}_3\text{C}_2\text{T}_x\text{-TBABr}$ and $\text{Ti}_3\text{C}_2\text{T}_x\text{-CTAB}$.

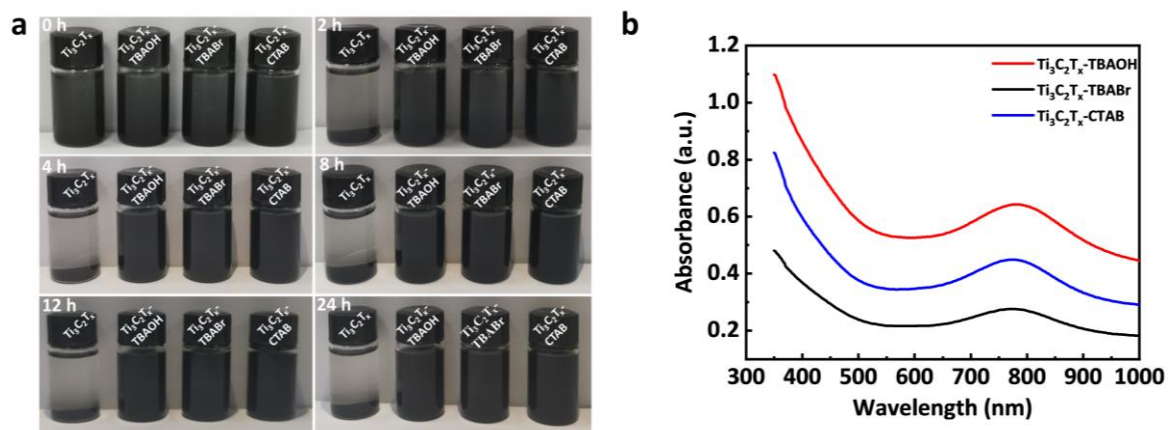


Fig. S3 (a) Dispersibility of $\text{Ti}_3\text{C}_2\text{T}_x\text{-TBAOH}$, $\text{Ti}_3\text{C}_2\text{T}_x\text{-TBABr}$, $\text{Ti}_3\text{C}_2\text{T}_x\text{-CTAB}$ in DMF; (b) The UV-vis-NIR absorption spectra after standing for 24 h.

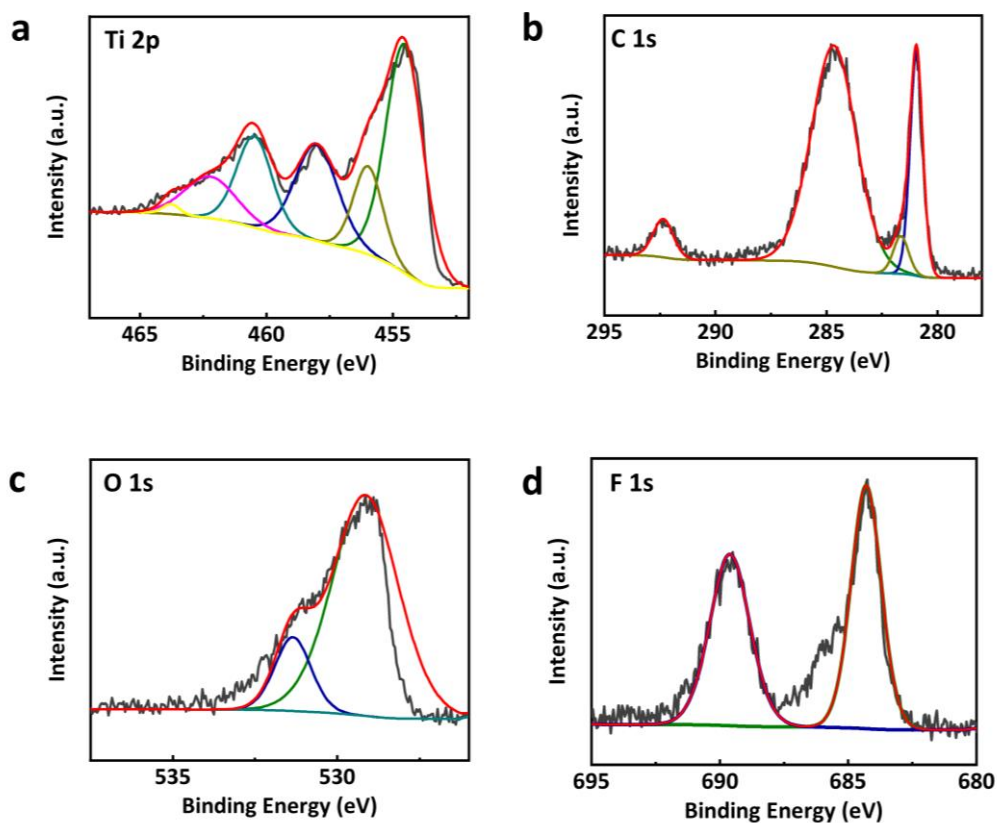


Fig. S4 High-resolved XPS spectra of Ti2p, C1s, O1s and F1s.

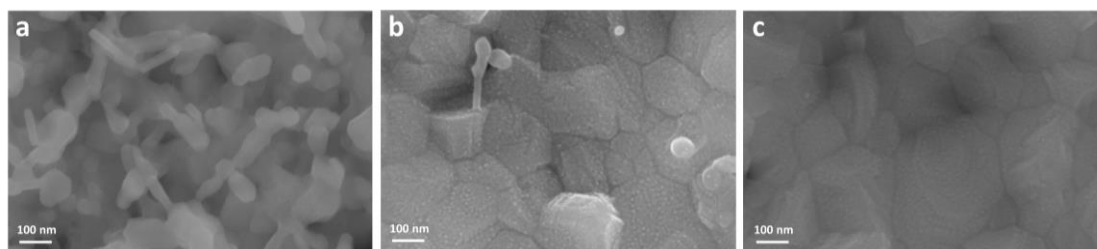


Fig. S5 Magnified SEM images of $\text{Ti}_3\text{C}_2\text{T}_x$ -TBAOH-modified perovskite film (a, 0wt%; b, 0.05wt%; c, 0.1wt%).

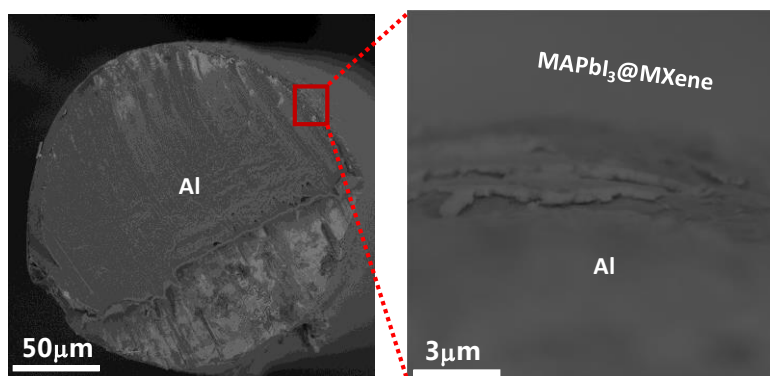


Fig. S6 Cross-sectional SEM images of $\text{Ti}_3\text{C}_2\text{T}_x$ -TBAOH-modified perovskite film.

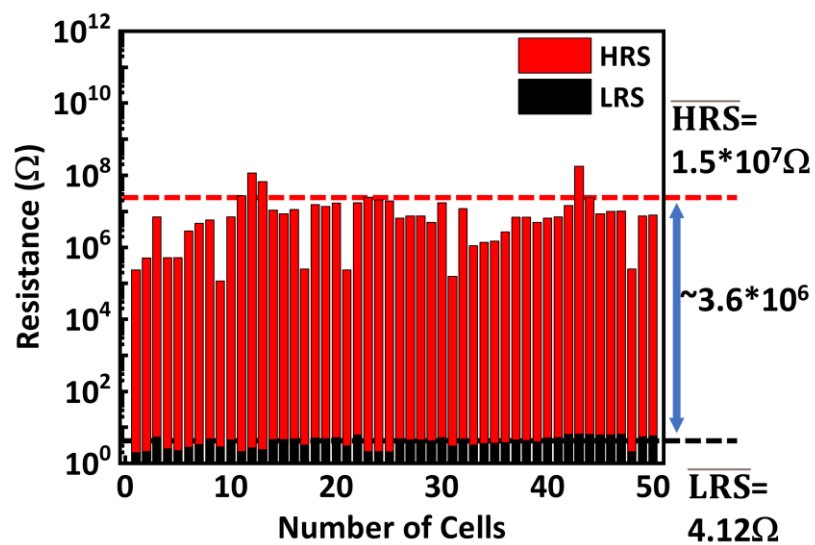


Fig. S7 HRS/LRS resistance for 50 pristine devices without the $\text{Ti}_3\text{C}_2\text{T}_x$ -TBAOH additive.

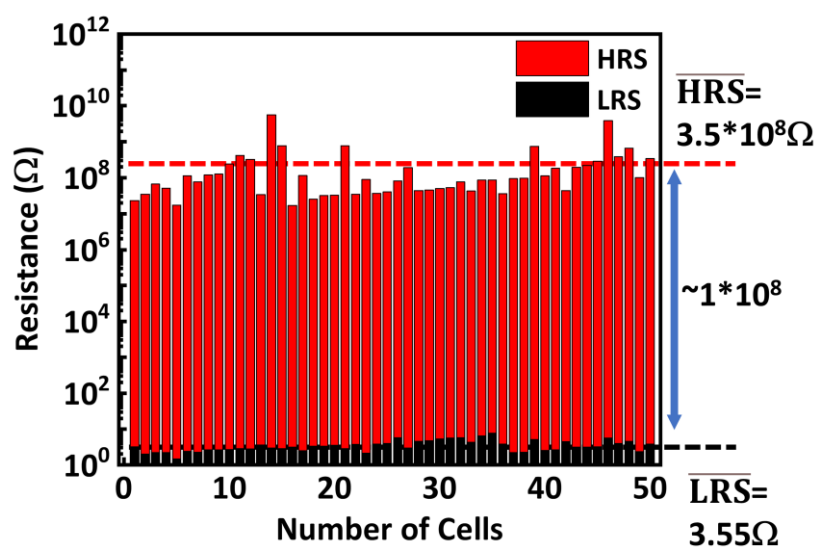


Fig. S8 HRS/LRS resistance for 50 $\text{Ti}_3\text{C}_2\text{T}_x$ -TBAOH-modified devices (0.1 wt%).

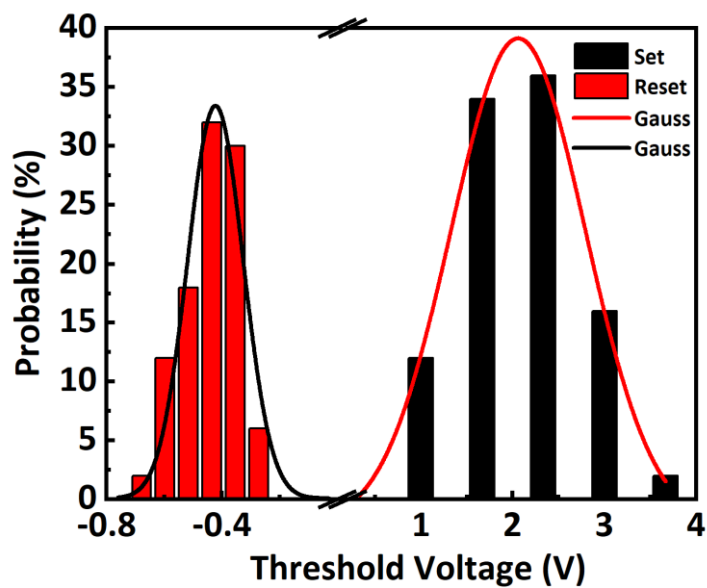


Fig. S9 Histogram of SET/RESET voltage of pristine devices without the $\text{Ti}_3\text{C}_2\text{T}_x$ -TBAOH additive.

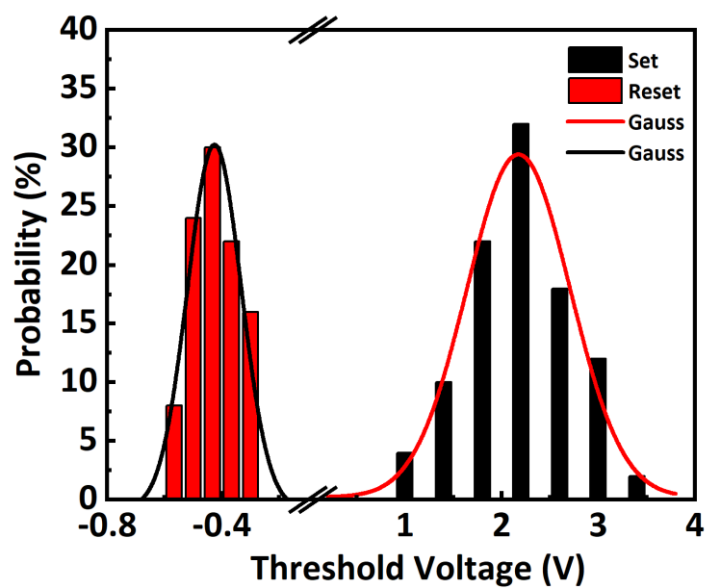


Fig. S10 Histogram of SET/RESET voltage of $\text{Ti}_3\text{C}_2\text{T}_x$ -TBAOH-modified devices (0.1 wt%).

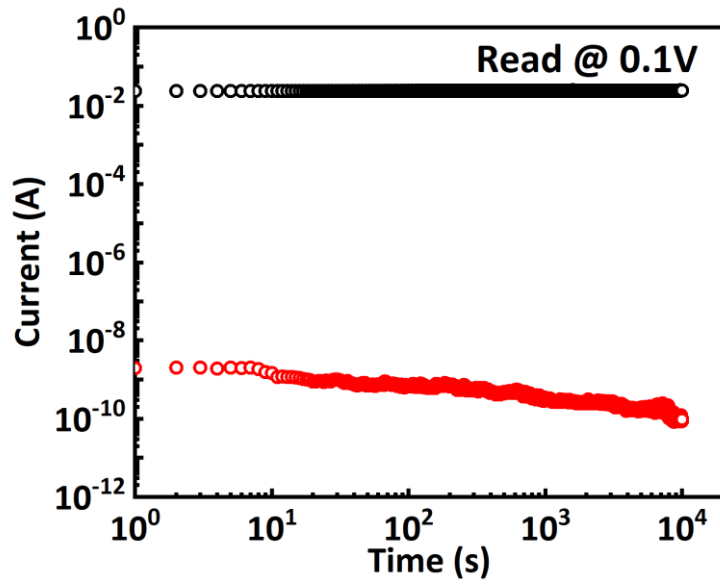


Fig. S11 Retention characteristics of pristine devices without the $\text{Ti}_3\text{C}_2\text{T}_x$ -TBAOH additive.

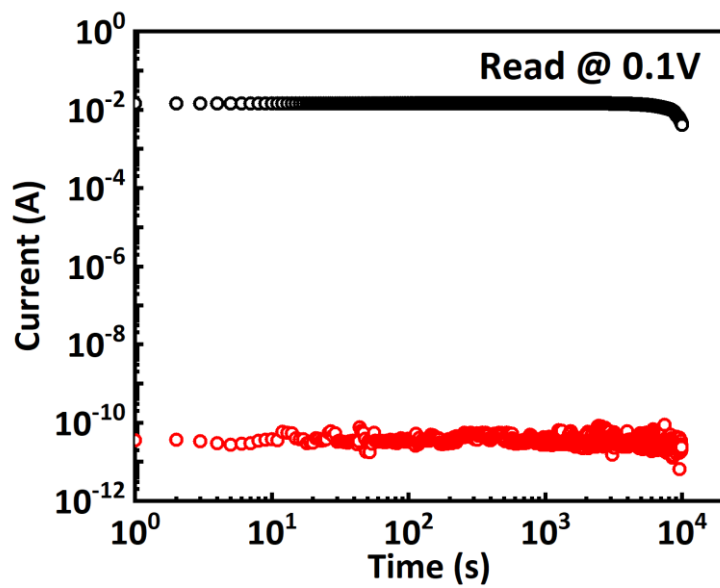


Fig. S12 Retention characteristics of $\text{Ti}_3\text{C}_2\text{T}_x$ -TBAOH-modified devices (0.1 wt%).

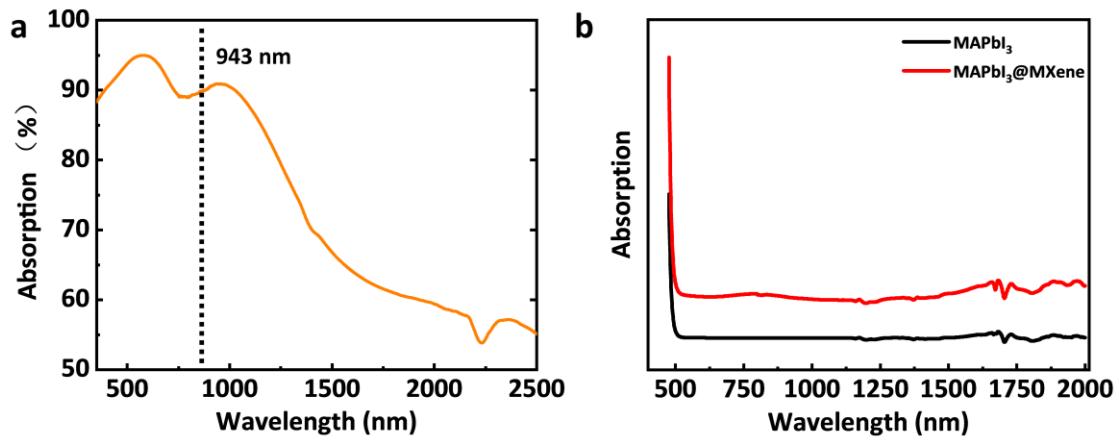


Fig. S13 UV-vis-NIR spectra of Ti₃C₂T_x-TBA powders (a) and MAPbI₃@MXene solution (DMF: DMSO= 4: 1, b).

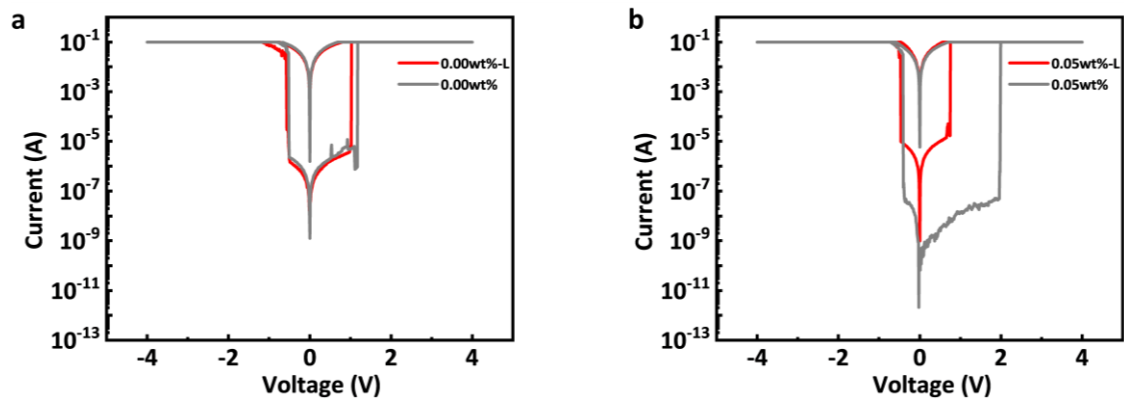


Fig. S14 I-V curves for pristine (a) and 0.1 wt% Ti₃C₂T_x-TBAOH-modified (b) devices in dark and under light irradiation.

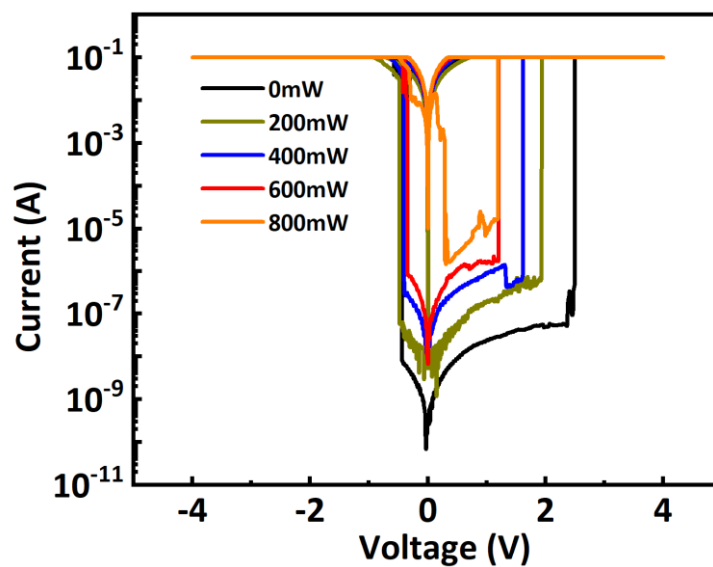


Fig. S15 I-V curves of 0.1 wt% Ti₃C₂T_x-TBAOH-modified RRAM device under illumination with different laser power.

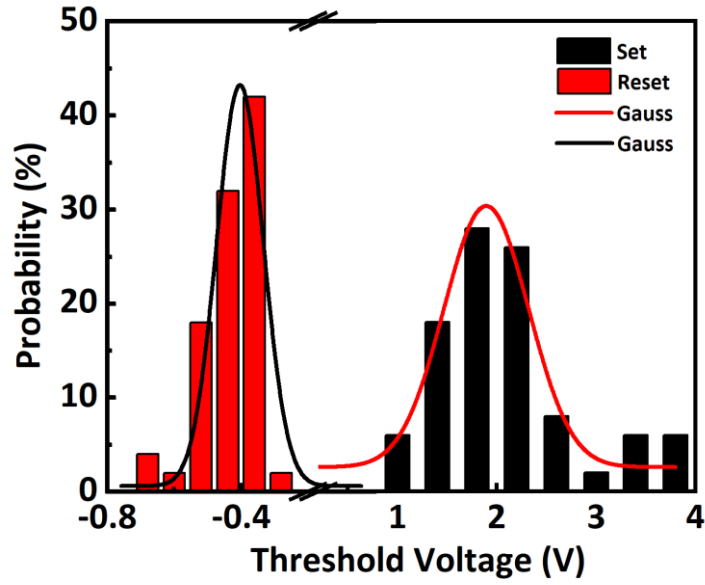


Fig. S16 Histogram of SET/RESET voltage of pristine devices under the NIR illumination.

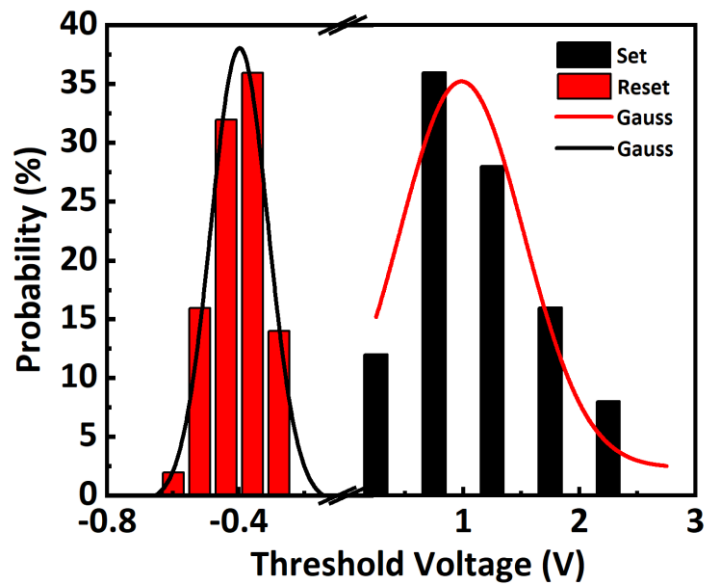


Fig. S17 Histogram of SET/RESET voltage of 0.1wt% $Ti_3C_2T_x$ -TBAOH-modified devices under the NIR illumination.

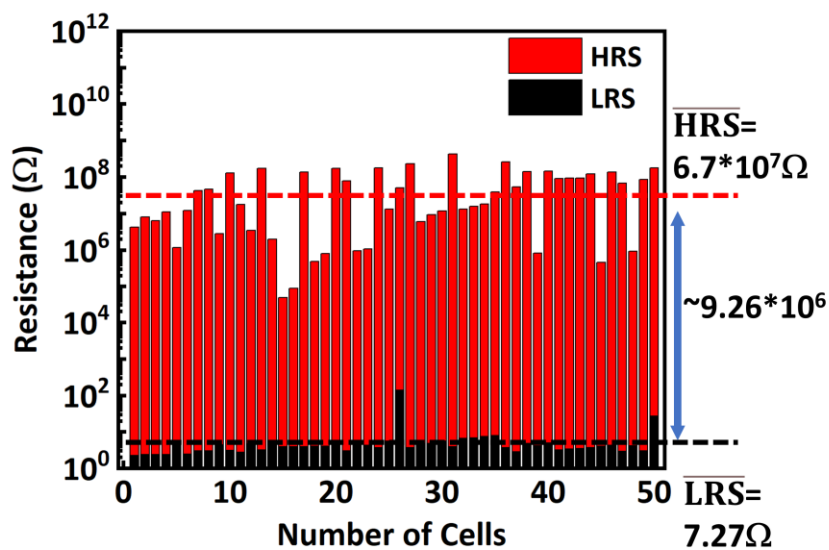


Fig. S18 HRS/LRS resistance for 50 pristine devices under the NIR illumination.

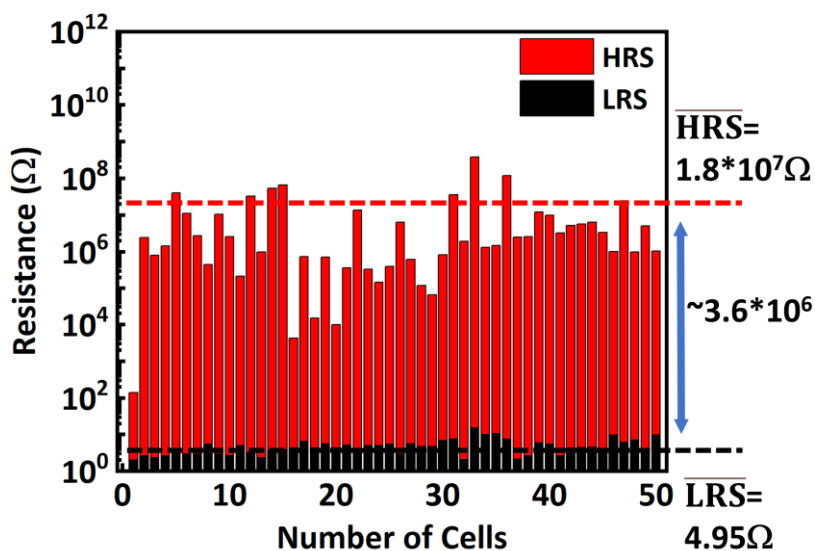


Fig. S19 HRS/LRS resistance for 50 $\text{Ti}_3\text{C}_2\text{T}_x$ -TBAOH-modified devices (0.1 wt%) under the NIR illumination.

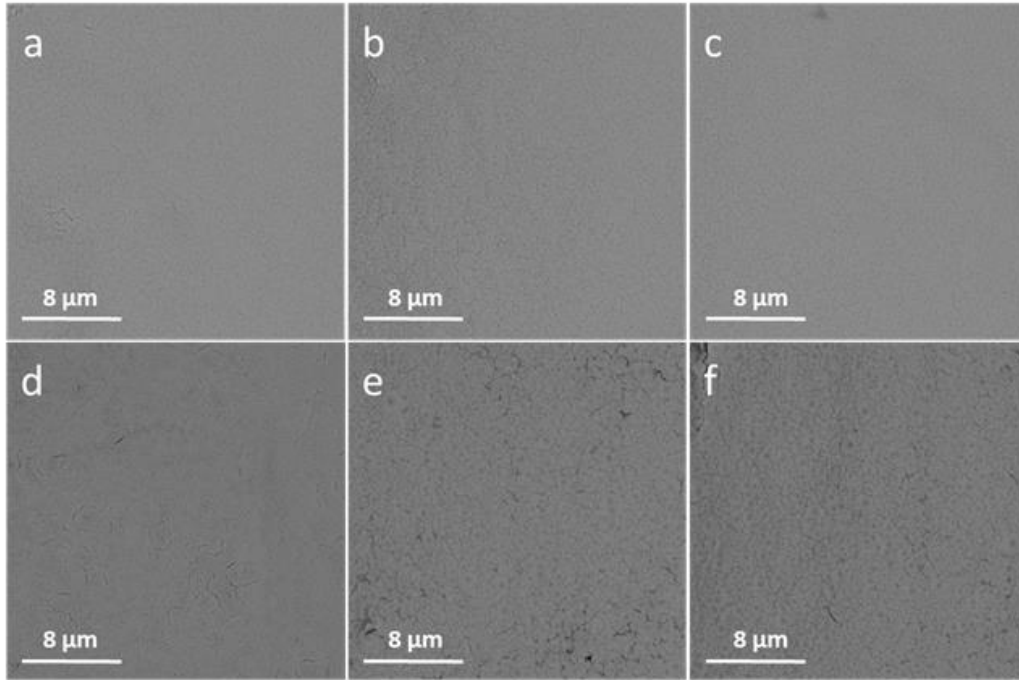


Fig. S20 SEM images of $\text{Ti}_3\text{C}_2\text{T}_x$ -TBAOH-modified perovskite film (a-c, before illumination; d-f, after illumination).